

ACMo: Attribute Controllable Motion Generation

Mingjie Wei¹ Xuemei Xie^{1†} Guangming Shi^{1,2}
¹Xidian University ²Peng Cheng Laboratory

mjwei@stu.xidian.edu.cn, xmxie@mail.xidian.edu.cn, gmshi@xidian.edu.cn

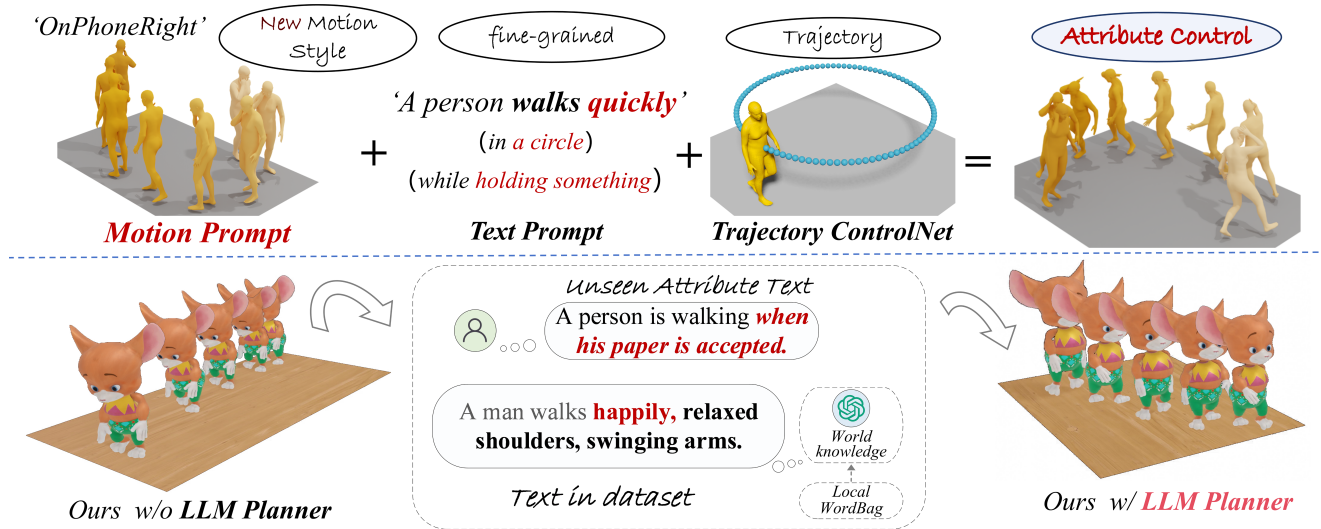


Figure 1. ACMo handles motions beyond dataset representation, using motion prompts for stylize multimodal generation and multi-attribute control, with LLM Planner mapping zero-shot unseen attributes to dataset texts. Employ rapid fine-tuning to enable the model to recognize new motion patterns. The bracketed text enhances the stability of style and trajectory. Control your motions as you wish!

Abstract

Attributes such as style, fine-grained text, and trajectory are specific conditions for describing motion. However, existing methods often lack precise user control over motion attributes and suffer from limited generalizability to unseen motions. This work introduces an Attribute Controllable Motion generation architecture, to address these challenges via decouple any conditions and control them separately. Firstly, we explored the Attribute Diffusion Model to improve text-to-motion performance via decouple text and motion learning, as the controllable model relies heavily on the pre-trained model. Then, we introduce Motion Adapter to quickly finetune previously unseen motion patterns. Its motion prompts inputs achieve multimodal text-to-motion generation that captures user-specified styles. Finally, we propose a LLM Planner to bridge the gap between unseen attributes and dataset-specific texts via local knowledge for user-friendly interaction. Our approach introduces the ca-

pability for motion prompts for stylize generation, enabling fine-grained and user-friendly attribute control while providing performance comparable to state-of-the-art methods. Project page: <https://mjwei3d.github.io/ACMo/>

1. Introduction

Motion generation from text and controllable signals offers a wide range of applications such as video games, animation production, virtual reality, and embodied robots. However, several key challenges hinder broader adoption: 1) Text inherently lacks granularity for precise motion control. 2) Real-world applications require handling unseen motion patterns beyond training data. For instance, "walk clockwise" produces semi-circle or full-circle paths, both valid but requiring control, while excessive text descriptions confuse models and reduce accuracy. Novel motion patterns (e.g., "elderly walking" or "when paper accepted") remain challenging without training or fine-tuning samples.

[†]Corresponding author

Table 1. Comparison of recent state-of-the-art method on diverse text-to-motion tasks. Our work achieves fine-grained and user-friendly controllable motion generation.

Methods	Attribute			Reason
	word-level	Style	Trajectory	
Momask [12]	✓	×	×	×
SmooDi [47]	×	✓	×	×
OmniControl [42]	×	×	✓	×
ChatPose [7]	×	×	×	✓
Ours	✓	✓	✓	✓

To address these issues, we propose to **decouple any conditions and control them** during the generation process. We analyze that motion is a combination of heterogeneous yet related features, such as action, motion style, and trajectory. Similarly, a text-to-motion description comprises key verbs (e.g., walk, jog, swim) and attributes (e.g., angry, arms uplifted, and clockwise). We aim to develop an end-to-end application for controllable stylized text-to-motion generation, effectively addressing the proposed challenges, as illustrated in Fig. 1. So, we design an Attribute Controllable Motion generation architecture called *ACMo* via plug-and-play modulars, which uses independent parameters to learn various conditional constraints. As shown in Tab. 1, it enables precise control in multimodal motion generation, including text, motion style, and trajectory.

Firstly, controllable generation relies on a high-performance text-to-motion pre-trained model [6, 42, 47]. It bridges the semantic gap between language and motion at word-level [12, 22] granularity. We propose to **decouple text and motion** modules to achieve a framework called *Attribute Diffusion Model (ADM)*, adopting continuous diffusion [5] rather than discrete autoregressive approaches [12, 20] for controlled generation. Three key innovations drive us: 1) We believe that decoupling using cross attention [18, 25, 37] is superior to feature concatenation [5], which provides better alignment. 2) However, the effect of cross attention is diminished in an over-compressed variational autoencoder (VAE). We attribute this to the inadequate motion representations due to the high performance of some vector-quantized representations [12, 20] in recent years. Therefore, we provide a more realistic motion VAE to preserve critical kinematic details. 3) The text encoder uses T5 [6, 31] instead of CLIP [34], as CLIP is object-based and struggles with actions and attributes. Experimental validation on HumanML3D [11] demonstrates that decoupling text-motion learning enhances performance for high-quality motion generation (FID reduced from 0.473 to 0.102), with inherent MultiModality benefits (2.614 exceeds 1.241).

Secondly, there is a precision paradox in text-motion alignment. Precise models are entrenched in the training data distribution, confined to narrow textual patterns, re-

stricting their capacity for open-instruction generalization. To address this, we propose an *LLM Planner* that mediates this generalization gap through reasoning, bridging dataset-specific text and unseen motion descriptions. It functions as an independent module to **decouple the text reasoning process**. Specifically, we implement three components: 1) Chain-of-Thought prompting [27, 48] for reasoning LLM (e.g. Deepseek-R1) with a high-frequency word knowledge, and 2) A zero-shot Motion Inference Text dataset called *MotionIT* featuring 5K high-level goal-driven motion descriptions for evaluation LLM Planner. 3) we developed a new evaluation system using LLMs. Thus, the planner enables user-friendly text-to-motion generation. It serves as a bridge for user interactions with model instructions, enhancing the model’s understanding of the desired actions.

Lastly, we **decouple styles and trajectories**, i.e. kinematics control signals, for controllable stylized generation. 1) Style: let the model ‘see’ the new *motion patterns* (e.g. motion style and new actions) and learn it. We attempt to simplify enabling motion prompts [43] for text-to-motion diffusion models. Thus, we design a *Motion Adapter* with motion prompt input, which can specify the required motion generation. The core idea is to allow the model to retain the original pattern knowledge and learn new motion patterns through **decoupling training**. We propose to reuse the decoupling modules of pre-trained model and fine-tune its corresponding modules to learn new motion patterns. This means that our motion prompt concretely generates semantics in the finetuning data. *This is a novel way to fine-tune new motion patterns, and very lightweight and fast training (15-20 minutes)*. We achieved great stylized motion generation on 100STYLE [30]. 2) Trajectory: following [6, 42], we adopted controlnet for trajectory control. Our focus is on verifying the compatibility between the motion adapter and ControlNet to achieve multi-attribute control.

In sum, our work has the following main contributions: 1) To the best of our knowledge, this is the first work to propose decoupling any condition and separately implementing multi-attribute text-to-motion generation. 2) The Motion Adapter is a lightweight, efficient fine-tuning method for multimodal motion generation, which achieves fine-tuning state-of-the-art on 100STYLE. 3) We leveraged LLMs to enable user-friendly text-to-motion generation, capable of handling previously unseen text inputs. 4) The Attribute Diffusion Model achieves performance on par with the state-of-the-art latent diffusion model on HumanML3D.

2. Related Work

Motion Generation generates 3D human motion sequences from multi-modal inputs, including image [21, 40], text [5, 11, 12, 20, 38, 46], action labels [3, 9, 32], audio [8, 26], control signals [6, 42], and incomplete pose sequences [14, 28]. In this paper, we focus on text and

control signals, with further distinction made between the fine-grained [4, 17, 22] content in the text and the trajectory and style [1, 19, 47] information in the control signals.

Text-to-Motion generation has gained significant attention in recent years. The mainstream approaches now learn shared latent representations to directly convert text into motion [9]. T2M [11] applied sequential VAEs [23] to learn the probabilistic relationship between motion and text. *Diffusion models* [16, 36] have significantly advanced this field, with MotionDiffuse [45] introducing the first text-based diffusion model. MDM [38] learned the mapping between text and motion in the original motion space. ReMoDiffuse [46] enhanced its performance by improving retrieval techniques. MLD [5] proposed learning the text-to-motion mapping in latent space, reducing noise and redundancy in long sequences. Additionally, some methods using VQVAE [39] and autoregressive models [12, 17, 20], such as MoMask [12] with residual codebook quantization, highlight the importance of latent motion representation. Following the previous discussion, we further explore the text-to-motion performance of the latent diffusion model.

Attribute Motion Control is implemented using a diffusion model, which has recently attracted attention due to its exceptional ability to control. ControlNet [44] enhances generative models by incorporating additional control inputs. Similarly, IP-Adapter [43] improves domain transferability through lightweight adapter layers. In motion generation, OmniControl [42] used spatial guidance and motion ControlNet to align generated motion with input trajectory signals. MotionLCM [6] introduced latent space consistency constraints to improve motion continuity. Our work focuses on seamlessly integrating trajectory control and motion style control. *Motion style* is elusive and hard to define mathematically, making data-driven approaches suitable for control and transfer. For instance, Aberman et al. [1] designed a two-branch pipeline to decouple and recombine motion styles, while Guo et al. [13] extract and infuse motion content and style in latent space. SmooDi [47] introduced style guidance and style ControlNet to direct motion, and MotionCLR [4] used an attention mechanism to edit motions without training. Compared to previous works, our approach conditions on motion style for multimodal control and uses lightweight adapters to refine the model.

LLM Planner for Motion Generation has gained increasing interest in recent years due to advances in large language models (LLMs). MotionGPT [20] finetuned T5 for unified tasks but lost text knowledge. ChatPose [7] was finetuned with reasoning generation but underperformed compared to specialized models. An AI agent [17, 24, 27, 48] to guide the LLM planner and integrate high-performance generative models can address these issues. For example, Xiao et al. [41] and Zhou et al. [48] used LLM as task planners for task decomposition. CoMo [17] uses ChatGPT

to get fine-grained text on different body parts. Inspired by this, we use the LLM to convert unseen text into training dataset-relevant text, achieving reasoning generation.

3. Method

We aim to address controllable motion generation with multimodal inputs. To generate a 3D pose sequence $\hat{m}_{1:L}$ of length L , with a motion prompt $p_{1:N}$ of length N , text condition c , and trajectory signal $s \in \mathbb{R}^{L \times J \times 3}$, we designed a novel attention-based motion latent diffusion model, as shown in Fig. 2. It decouples style, and trajectory training across the network: first, training the text-to-motion Attribute Diffusion Model, then finetuning the Motion Adapter for stylized motion prompt inputs, and finally integrating Trajectory ControlNet for spatial signal control.

3.1. Training: Attribute Diffusion Model

Inspired by [4, 5, 12, 18], we designed the Attribute Diffusion Model (ADM) in the latent space. This model leverages a transformer-based architecture [5, 32], consisting of a Motion Variational AutoEncoder, text embeddings, and the Attribute Latent Diffusion Model.

Motion Variational AutoEncoder consists of a motion encoder \mathcal{E} and a motion decoder \mathcal{D} , trained solely on motion sequences $m_{1:L} \in \mathbb{R}^{L \times H}$ without text, where $H = 263$ denotes the dimension of motion representation. We adopted a transformer-based architecture in the MLD [5] for Motion VAE, adjusting the network parameters to enhance the codec’s performance. This VAE codec has lower computational overhead and produces more diverse motions. Specifically, the low-dimensional vectors are in motion latent space $z = \mathcal{E}(m)$, then reconstructed by decoder $\hat{m} = \mathcal{D}(z)$. The Mean Squared Error (MSE) loss and the Kullback-Leibler (KL) divergence are used as losses for reconstructing the training motion.

Text Embedding maps textual descriptions to the latent space. Most previous work [5, 12, 17] relied on CLIP as a text encoder, but its focus on object-level text limits fine-grained property descriptions. Instead, we used T5 [31] for text embedding τ , achieving improved performance.

Attribute Latent Diffusion Model aims to explore a more powerful motion diffusion model in latent space. The diffusion probabilistic model [16] transforms Gaussian noise into a data distribution $p(x)$. Its forward process is a Markov chain that gradually adds noise over k steps, while the reverse process anneals the noise by modeling the conditional noise ϵ . Specifically, the process initializes with a latent vector $z_0 \in \mathbb{R}^{L \times D}$ from Motion VAE. Through forward diffusion, noise is systematically introduced across k time steps, progressively transforming z_0 into a noisy latent state z_k . This formulation permits closed-form sampling at

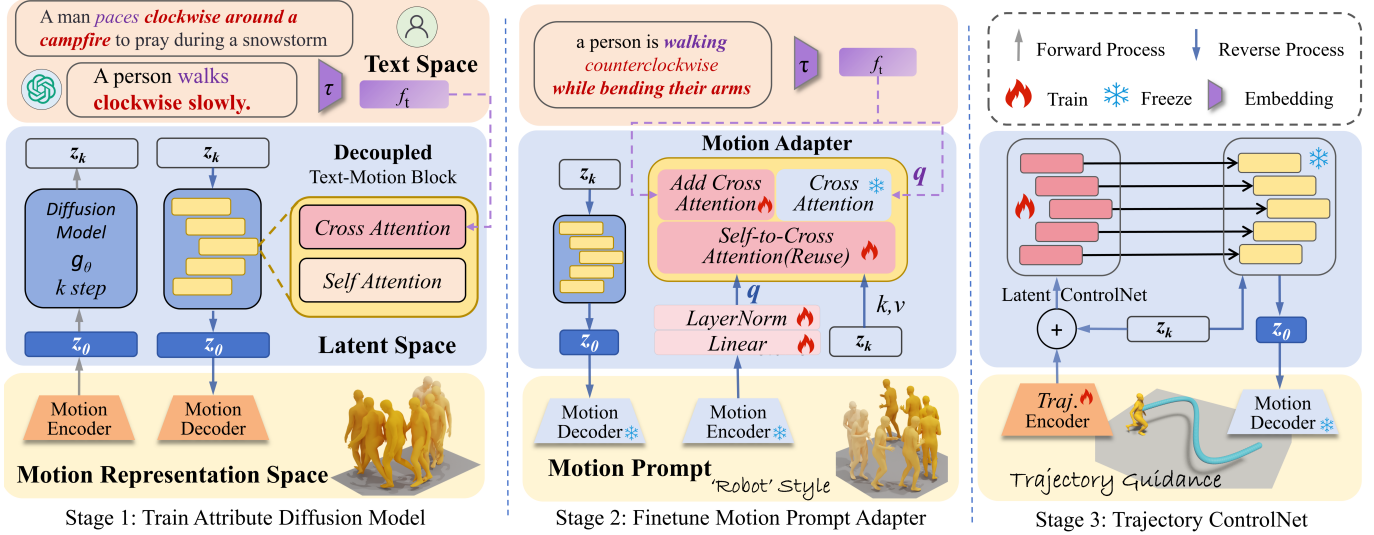


Figure 2. The ACMo network architecture. Stage 1: *Attribute Diffusion Model* is trained by decoupling text and motion in a more powerful latent space. Stage 2: *Motion Adapter* finetunes new motion patterns and preserves the original knowledge. Stage 3: Trajectory control through ControlNet. Finally, the LLM Planner module inferences for text processing.

arbitrary step k via:

$$q(z_k|z_{k-1}) := \mathcal{N}(z_k; \sqrt{\alpha_k}h_0, (1 - \alpha_k)I), \quad (1)$$

where $\alpha_k \in (0, 1)$ denotes a hyper-parameter for sampling. The reverse diffusion step is expressed by the trained diffusion model g and its parameters θ as follows:

$$z_{k-1} = g_\theta(z_k, f_t), \quad k \in \{1, \dots, K\}, \quad (2)$$

where f_t represents the conditional text feature at each diffusion step based on the predicted noise $\epsilon \sim \mathcal{N}(0, 1)$.

Our denoiser g_θ (parameterized by θ) builds upon MLD [5] and all layers with long skip connections [2]. We designed the text-motion block to implement our denoiser using stacked self-attention and cross-attention. *Self Attention* layers model the relationship between motions themselves without text condition [4, 5, 38]:

$$z = \text{Attn}(q, k, v) = \sigma(qk^T/\sqrt{d})v, \quad (3)$$

where q , k , and v represent the query, key, and value, respectively, all corresponding to the motion modality, and $\sigma(\cdot)$ denotes the softmax function. *Cross Attention* layers model the relationship between different decoupled multi-modal data in latent space. In text-to-motion tasks, they model the correlation between text and motion sequences [18]. It can be formulated as:

$$\text{CrossAttn}(q, k', v') = \sigma(qk'^T/\sqrt{d})v', \quad (4)$$

where q represents the text feature, and k' and v' are the motion latent vectors.

3.2. LLM Planner

LLM Planner serves as an independent plug-and-play module in our framework. The planner enhances text descriptions via zero-shot text inference. We tried different large language models in Sec. 4.3, both easy to deploy and commercially available. Additional details about the prompt are provided in the supplementary.

Inspired by the proposed precision paradox, we made a wordbag as local knowledge. *The higher the frequency of words in the dataset, the better the alignment performance.* We constructed the proposed local knowledge base by relying on TF-IDF [35] to calculate the importance of all texts in the dataset, and then selected the most important 512 words as local knowledge. This allows the model to map unseen text to text in the dataset. Finally, we have developed an evaluation system for assessing the results of LLM Planner by leveraging another LLM as an evaluator in Sec. 4.

3.3. Fineture: Motion Prompt Adapter & Trajectory ControlNet

Inspired by [4, 42, 43, 47], we propose a lightweight finetuning method to learn new motion patterns. Our model is characterized by the fact that we reuse the decoupling module of ADM and finetune its corresponding modules to learn new motion patterns.

Decoupled Fineture. Because different motions are new patterns with the same representation. We freeze and reuse motion VAE in the fine-tuning process, unlike other motion style training methods [47]. In Sec. 4.4, we designed experiments to verify that the decoupling method (c) in Fig. 3 can

efficiently learn the motion patterns with a small amount of data and training while retaining the text knowledge.

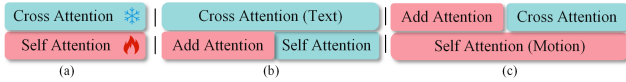


Figure 3. To achieve retaining text knowledge, we froze decoupled cross attention. Three fine-tuning methods are carried out, and the method (c) achieved the most efficient learning of motion patterns.

Decoupled Additional Text Cross Attention. In order to preserve the original knowledge, we used a new cross attention to complement the new textual and visual mapping. We train the decoupled cross attention in Fig. 3 and then add it to the original cross attention [43]. It can be formulated as:

$$z^{new} = \sigma(qk^T/\sqrt{d})v + \sigma(qk'^T/\sqrt{d})v', \quad (5)$$

where q represents the text feature, k' differs from k by $k = zW$ and $k' = zW'$, with W' being the weight matrix of the additional attention. The same applies to v .

Self-to-Cross Attention. Inspired by [4, 43], to achieve a function similar to motion style transfer, we propose to utilize motion prompts for multimodal stylized text-to-motion generation. With motion prompts, fine-grained and specific stylized results can be obtained within the specified text range. As shown in Stage 2 of Fig. 2, we added a linear layer and layer norm on Fig. 3 (c) to linearly transform the latent vectors. Self-to-cross attention refers to turning a self attention query in Eq. 3 into a motion prompt to achieve cross attention. This can be formulated with Eq. 4, where q is a motion prompt latent vector.

Trajectory ControlNet. We build and only use trajectory ControlNet to address the trajectory control, following [6, 42]. Our core goal is to verify the compatibility of the trajectory controlnet with our motion adapter, so we set the hip controls for simplicity. We achieve this by copying denoiser g in Stage 1 and adding it with a zero-initialized linear layer for eliminating random noise. Trajectory control is learning by training the trajectory encoder and ControlNet. Details are provided in the supplementary.

4. Experiment

Dataset. First, we train and evaluate the proposed Attribute Diffusion Model on the popular text-to-motion dataset, *HumanML3D* [11]. It collects 14,616 motion sequences and each motion was annotated with text from AMASS [29] and HumanAct12 [10]. Thanks to [47], we use *100STYLE* [30] to finetune our Motion Adapter. Lastly, we present our evaluation dataset of the LLM Planner on MotionIT dataset (Sec. 4.1).

Evaluation metrics are followed as per [5, 12, 20, 47, 48]. (1) Motion Quality: The Frchet Inception Distance

(FID) compares feature distributions between real and generated motions via feature extractor [11]. (2) Condition Matching: R-Precision (Top-1/2/3 accuracy) and Multimodal Distance (MMDist) to assess text-motion alignment. (3) Diversity is measured by Diversity (DIV, feature variance) and MultiModality (MModality, diversity within same text input). (4) LLM Planner evaluation: Metrics such as Bleu, Rouge, and Cider assess the performance. Inspired by [48], we propose a evaluation framework via LLM with differentiated prompts for Rule Consistency Score (RCS) and Plan Score (PS). $RCS \in \{0, 1\}$ checks rule compliance, and $PS \in [1, 5]$ rates planning rationality. (5) Average Response Time (ART) measures the LLM’s average time per instruction.

Traning Detail. Training loss and classifier-free diffusion guidance [15] are constructed according to MLD [5]. The optimization objective of the proposed model is:

$$L_{ADM} := \mathbb{E}_{g,t} \left[\|\epsilon - g_\theta(z_t, t, c)\|_2^2 \right], \quad (6)$$

where ϵ denotes the noise generated in the forward process; c is the conditions, *i.e.* texts f_t , motion prompt f_m and trajectories f_{tra} ; t denotes the diffusion steps, we freeze the text encoder τ [33] and optimize the diffusion model g .

Implementation Details. Our denoiser g_θ in Sec. 3.1 employs 11 layers and 4 attention heads, with GELU as the activation function. A frozen Sentence-T5-large serves as the text encoder. The latent representation has a shape of $z \in \mathbb{R}^{7,256}$. All models are trained using the AdamW optimizer with a fixed learning rate of 10^{-4} and a mini-batch size of 128. Other key model configurations, such as the number of layers and guidance scale in the diffusion model, are analyzed in the ablation study (Sec. 4.2). Training the Attribute Diffusion Model takes approximately 48 hours, and VAE training 30 hours on $2 \times A6000$ GPUs. Training motion adapter takes *only 15 minutes* to train 100 epochs. Additional experimental details can be found in the supplementary materials.

4.1. Motion inference text dataset for LLM Planner

Motion represents goal-driven human pose expressions. We created MotionIT to evaluate the LLM Planner on reasoning motion generation. It tests zero-shot inference capabilities for open-instruction requirements. The dataset includes everyday situations, emotional states, intentional goals, and time-sensitive actions, focusing on context-aware motion through scenario narratives and environmental dynamics.

Simple cases include “A person jogs to catch a bus pulling away from the stop.” while complex ones involve reasoning about emotions or interactions, like “A person checks their bank balance, wondering if they can afford to take a financial risk.” Moreover, we incorporate lengthy narrative sequences. While MotionIT presents challenging in-

Table 2. Comparison of text-conditional motion synthesis on HumanML3D. We evaluate each metric 20 times. "↑" indicates higher is better, "↓" indicates lower is better, and "→" indicates closer to real motion is optimal. All methods use the ground truth motion length and are sorted by FID. **Bold** and *italic* denote the best and second best results, respectively. (†) denotes a diffusion-based method. MLD is our baseline for ablation. We ablated the effectiveness of the entire module with 9 layers, achieved optimal performance with 11 layers. The proposed ADM achieve *comparable FID and R Precision*, with **MModality** being a notable advantage. The proposed method is of particular significance as it is not only an accurate improvement, but also inherently **controllable** in latent space.

Methods	R Precision↑			FID↓	MM Dist↓	Diversity→	MModality↑
	Top 1	Top 2	Top 3				
Real	0.511±.003	0.703±.003	0.797±.002	0.002±.000	2.974±.008	9.503±.065	-
T2M [11]	0.457±.002	0.639±.003	0.740±.003	1.067±.002	3.340±.008	9.188±.002	2.090±.083
MotionDiffuse (†) [45]	0.491±.001	0.681±.001	0.782±.001	0.630±.001	3.113±.001	9.410±.049	1.553±.042
MDM (†) [38]	0.418±.005	0.604±.005	0.707±.004	0.489±.025	3.630±.023	9.450 ±.066	2.870 ±.111
MotionLCM (†) [6]	0.502±.003	<i>0.698</i> ±.002	<i>0.798</i> ±.002	0.304±.012	3.012±.007	9.607±.066	2.259±.092
CoMo [17]	0.502±.002	0.692±.007	0.790±.002	0.262±.004	3.032±.015	9.936±.066	1.013±.046
MotionGPT [20]	0.492±.003	0.681±.003	0.778±.002	0.232±.008	3.096±.008	9.528 ±.071	2.008±.080
ReMoDiffuse (†) [46]	<i>0.510</i> ±.005	<i>0.698</i> ±.006	0.795±.004	0.103±.004	2.974±.016	9.018±.075	1.795±.043
MoMask [12]	0.521 ±.002	0.713 ±.002	0.807 ±.002	0.045 ±.002	2.958 ±.008	9.648±.066	1.241±.040
MLD (†) [5]	0.481±.003	0.673±.003	0.772±.002	0.473±.013	3.196±.010	9.724±.082	2.413±.079
Ours (ADM)	0.493±.002	<i>0.698</i> ±.003	0.795±.002	<i>0.102</i> ±.003	<i>2.973</i> ±.006	9.749±.082	<i>2.614</i> ±.100
+ VAE-7	0.473±.004	0.667±.003	0.769±.003	0.305±.011	3.159±.009	9.663±.072	2.460±.104
+ VAE-7 & T5	0.478±.002	0.680±.003	0.785±.002	0.265±.009	3.086±.008	9.827±.089	2.447±.099
+ VAE-7 & T5 & CrossAttn	0.486±.003	0.687±.003	0.791±.003	0.122±.005	3.044±.011	9.670±.070	2.532±.095

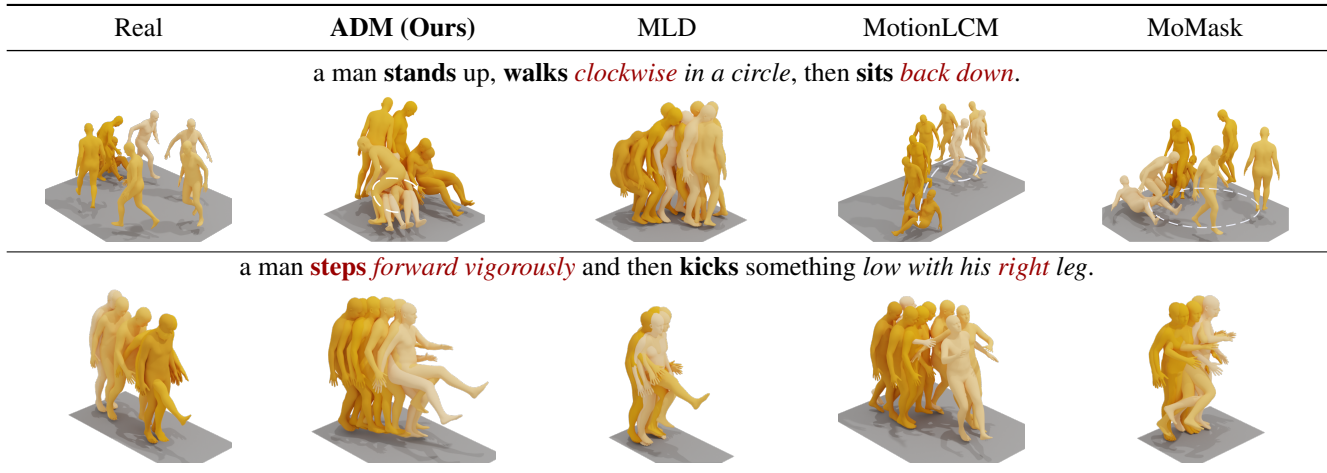


Figure 4. Visualization Comparison between the different methods given two distinct text descriptions from HumanML3D testset. **Bold** and *italic* denote the verb and attribute, respectively. This visualizes **subtle differences** at the word level, which illustrates the advantages of our approach.

structions, the LLM Planner offers a suboptimal but executable solution.

4.2. Text-to-motion generation Experiment

Comparison experiment are evaluated as shown in Tab. 2. The proposed ADM is compared the state-of-the-art methods on HumanML3D. Firstly, the improvement of our method over the baseline [5] is significant. Compared with all current diffusion model [5, 6, 38, 45, 46] methods, our method achieves the best performance. Importantly, our

method has a high MModality advantage while reducing the FID. We observed that this is also a characteristic of diffusion models and realistic VAEs. Although it is slightly inferior in performance compared to autoregressive models [12], our method has unique controllability and style learning capabilities. In the supplementary materials regarding the comparison between VAE and existing methods, the VAE-7 we designed has achieved the best performance. **Visualization** of text-to-motion can be seen in the Fig. 4.

Ablation Studies. *Component Analysis* is presented in

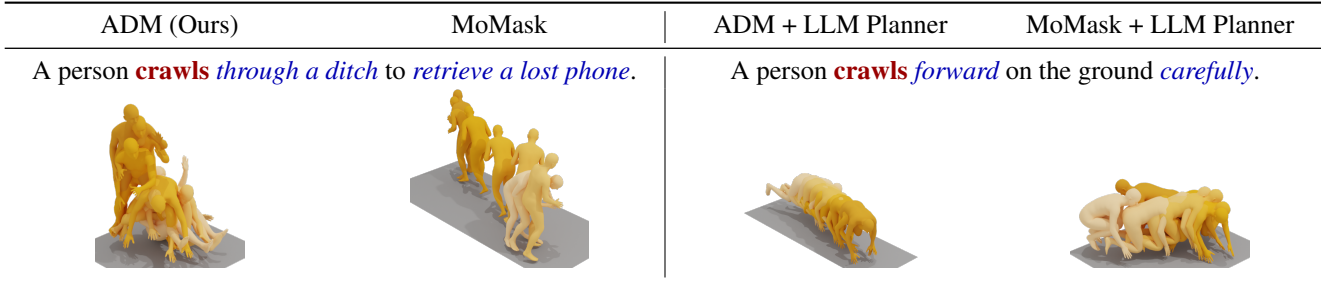


Figure 5. Visualization LLM Planner example. **Bold** and *italics* represent key verb and the transformation of the inference context, respectively. The model struggles with understanding context and gets disturbed (e.g., 'retrieve' as a goal not a generated action) without LLM planner. The LLM understands user instructions and leverages world and local knowledge to convert into dataset text (e.g., 'through a ditch' \rightarrow 'forward' and 'retrieve a lost phone' \rightarrow 'carefully'), enabling effective diffusion model generation.

Tab. 2, which includes the ablation effects of three main components. This clearly highlights the significant performance improvements achieved through our decoupled optimization of text and motion modalities. A more realistic VAE (i.e. VAE-7) and a higher-performing diffusion model can achieve better alignment effects. *Cross Attention* added significantly improved performance, particularly in the powerful latent space. Therefore, we conducted ablation experiments in Tab. 3. Obviously, our two designs have been improved compared with no cross attention. We have verified the two designs: Stack Layers which learn motion first and then align it with text, and Blocks which learn motion relationships and align it while learning motion, which shows that our Block design is more efficient. To further understand its impact, we conducted an ablation study on its parameters, including the number of layers and guidance scale. We optimize the model for complex latent space capabilities by increasing the number of model layers. By adjusting the train-free hyperparameters, we can obtain models with different characteristics. In conclusion, the ablation experiments demonstrate the effectiveness of cross attention in latent space.

Table 3. Ablation of Cross Attention layers on HumanML3D. GS represents guidance scale, which is a train-free hyperparameter. The number of network layers in our experimental design and GS is 9 and 11, respectively.

Methods	R Precision Top 1 \uparrow	FID \downarrow	MM Dist \downarrow	Diversity \rightarrow	MModality \uparrow
Real	0.511 \pm .003	0.002 \pm .000	2.974 \pm .008	9.503 \pm .065	-
w/o Attn.	0.478 \pm .002	0.265 \pm .009	3.086 \pm .008	9.827 \pm .089	2.447 \pm .099
Stack layer	0.480 \pm .002	0.149 \pm .005	3.080 \pm .007	9.737 \pm .075	2.605 \pm .010
Block	0.486 \pm .003	0.122 \pm .005	3.044 \pm .011	9.670 \pm .070	2.532 \pm .095
Block (5 layers)	0.438 \pm .003	0.242 \pm .006	3.279 \pm .008	9.726 \pm .088	2.790 \pm .113
Block (7 layers)	0.471 \pm .002	0.153 \pm .006	3.119 \pm .007	9.687 \pm .087	2.674 \pm .098
Block (9 layers)	0.486 \pm .003	0.122 \pm .005	3.044 \pm .011	9.670 \pm .070	2.532 \pm .095
Block (11 layers)	0.492 \pm .002	0.113 \pm .005	3.034 \pm .006	9.785 \pm .085	2.566 \pm .095
Block (13 layers)	0.478 \pm .002	0.109 \pm .004	3.077 \pm .007	9.813 \pm .077	2.549 \pm .081
GS = 6.5	0.493 \pm .002	0.102 \pm .003	2.973 \pm .006	9.749 \pm .082	2.614 \pm .100
GS = 7	0.489 \pm .002	0.107 \pm .003	3.050 \pm .006	9.739 \pm .075	2.517 \pm .078
GS = 7.5	0.492 \pm .002	0.113 \pm .005	3.034 \pm .006	9.785 \pm .085	2.566 \pm .095
GS = 8	0.485 \pm .003	0.103 \pm .004	3.064 \pm .007	9.726 \pm .073	2.554 \pm .080
GS = 8.5	0.497 \pm .003	0.121 \pm .005	3.017 \pm .007	9.795 \pm .090	2.503 \pm .093

It is worth noting that our experimental results are inconsistent with, or even contrary to, the results of MLD [5]. MLD believes that the insufficient performance of VAE-7 is due to insufficient data. However, we proposed that the stronger Motion VAE requires a more powerful latent diffusion model to achieve better text alignment. This is achieved through cross attention and the addition of layers. Therefore, cross attention will perform worse in an insufficient latent space (VAE-1), and VAE-7 will perform worse in the absence of a more powerful diffusion model.

4.3. Reasoning motion generation Experiment

We conducted a visualization experiment, as shown in Fig. 5. It can be seen that through the LLM Planner, unseen zero-shot texts can be converted into dataset descriptions, thereby facilitating user-friendly motion generation.

LLM Planner Ablation. In Tab. 4, we conduct experiments directly using prompt engineering on the Llama, Qwen, and Deepseek models. In our experiments, we found that Deepseek-r1 performs best, effectively enabling the diffusion model to understand dataset-specific text and complete inference generation. However, its response time for each instruction is slow due to the reasoning chain process. Meanwhile, other current large models can also perform this task effectively. We recommend using Deepseek-V3 or Qwen2.5-max as an LLM Planner for tradeoff.

Table 4. Ablation of LLM Planner on MotionIT. We used original instruction in MotionIT as ground truth for BLEU, ROUGE, and CIDEr. A DeepSeek-R1-Distill-Qwen-32B acts as a judge to calculate the PS and RCS. We take samples and repeat the tests on the samples three times.

Method	BLEU@4 \uparrow	ROUGE \uparrow	CIDEr \uparrow	PS \downarrow	RCS(%) \uparrow	ART \downarrow
Deepseek-R1	0.04	0.27	0.13	3.37 \pm .04	75 \pm 2	63.04s
Deepseek-V3	0.08	0.44	0.62	2.16 \pm .04	59 \pm 1	2.49s
Qwen2.5-max	0.14	0.52	1.21	1.55 \pm .04	55 \pm 1	856ms
llama-3.2-3B	0.04	0.27	0.17	3.42 \pm .06	40 \pm 1	13.96ms
llama-3.2-1B	0.06	0.32	0.33	4.50 \pm .03	37 \pm 1	13.57ms

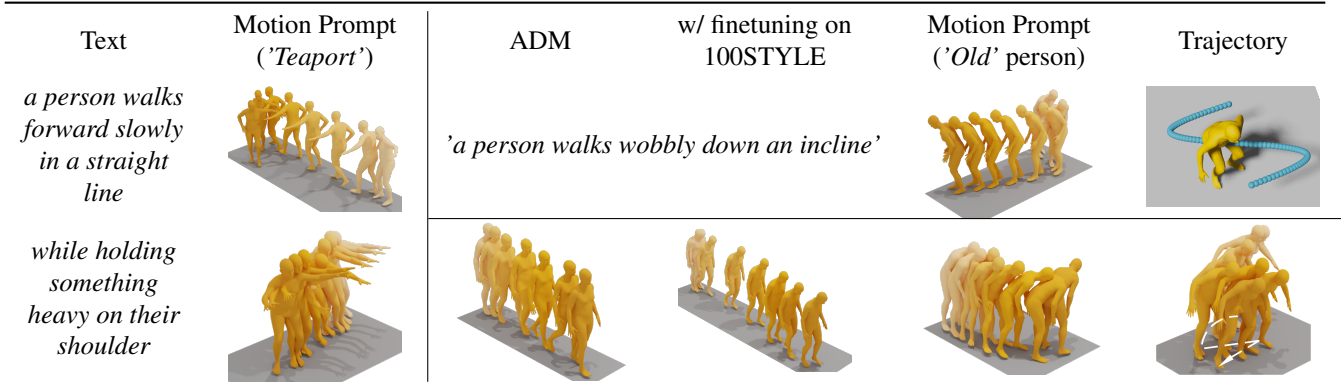


Figure 6. Visual ablation experiment of motion prompt and trajectory. The proposed Motion Adapter facilitates stylized generation by motion prompts to specific semantics, as shown on the left. On the right is a visualization example of multiple attributes without enhanced text description, we finetune then add a motion prompt, and subsequently add a track. More visualizations in supplemental material.

4.4. Motion Style and Trajectory Experiment

To ensure a fair comparison and eliminate the influence of data factors, we used the model without the LLM Planner for attribute experiments. Except for Fig. 1, additional visualization examples are provided in Fig. 6. This shows the effect of the proposed multiple attribute controls. We use the *motion prompt* to specify the motion we wish, allowing the model to understand the motion to be generated under the text category.

Table 5. Comparison of text-to-motion generation on 100STYLE via finetuning. *Param.* represents the sum of the number of frozen parameters and the number of *trainable* parameters. Text data annotated via MotionGPT [20] lacks adequate 'Real' motion description. The FID metric measures the difference in data distribution between the generated results and 100STYLE motions, which is important. Finetuning training within 100 epochs.

Dataset	Methods	R Precision Top 3 \uparrow	FID \downarrow	MM Dist \downarrow	Diversity \rightarrow	Param. (M)
w/o finetune	Real (100STYLE)	0.317 \pm .004	-	5.687 \pm .026	6.492 \pm .066	-
	MLD	0.687 \pm .007	5.956 \pm .114	3.610 \pm .029	9.102 \pm .071	8.3
	ADM	0.766 \pm .006	5.935 \pm .109	3.109 \pm .019	8.960 \pm .066	20.3
	Smoodi [47]	0.571	1.609	4.477	9.235	8.3+19.2
100STYLE	ADM (Full Model)	0.539 \pm .008	1.223 \pm .055	4.527 \pm .028	7.468 \pm .083	+20.3
	Motion Adapter	0.597 \pm .007	1.271 \pm .055	4.217 \pm .024	7.361 \pm .060	10.6+19.2
	Add on Self Attn.	0.591 \pm .009	2.095 \pm .124	4.099 \pm .033	7.830 \pm .088	20.1+ 9.7
	Only train Self Attn. (epoch=1000)	0.597 \pm .008	1.800 \pm .066	4.120 \pm .030	7.897 \pm .077	11+ 9.7
	+ Add on Text Attn.	0.487 \pm .007	0.887 \pm .066	4.841 \pm .036	7.205 \pm .069	11+ 9.7
	+ Add on Text Attn.	0.576 \pm .007	1.486 \pm .060	4.264 \pm .035	7.679 \pm .094	10.6+19.2
	+ Self-to-Cross Attn.	0.597 \pm .007	1.271 \pm .055	4.217 \pm .024	7.361 \pm .060	10.6+19.2

Motion Adapter Ablation. We attempted to achieve fine-tuning with new motion patterns, as shown in Tab. 5. Overfitting is prevented within 100 epochs. The FID of the ground truth compared to itself is less than $1e-9$ and can be considered negligible. Firstly, since our text auto-annotations come from MotionGPT [20], this is not a high-quality labeled and may cause confusion with previous data, thus reducing R Precision. Secondly, we hope to learn new motion patterns while retain the original training

knowledge. So, it is obviously that our method reduces the value of FID while retaining the R precision. This is a significant advantage of our decoupling training, our method don't forget the original text memory. At the same time, our method has very few training parameters and fast training. In contrast, the parameters of ControlNet in Smoodi relies on the denoiser of replicated pretrain model. Despite the ADM having more parameters than MLD, the motion adapter requires fine-tuning only a minimal set of parameters to achieve superior performance, highlighting its efficiency. Our method solves three issues: 1) MLD's weak text-to-motion ability, 2) the 10x longer training time compared to MLD in Smoodi [47] and 3) maintain knowledge then learn new patterns. Finally, the proposed approach enables rapid fine-tuning to allow the model to 'see' new motion patterns.

5. Discussion and Conclusion

Discussion. Generating motion trajectories from text and fine-tuning new actions via video will be our future work. Meanwhile, existing metrics are inadequate, such as the absence of quantitative evaluation for multi-attribute tasks and cases where R Precision exceeds real motion data. Finally, we believe that the proposed motion adapter and decoupling any conditions can provide insights for the generation of images, videos, and 3D models.

Limitations. We acknowledge certain limitations in ACMo. The text-to-motion latent diffusion model offers ease of control but is less precise than state-of-the-art. Additionally, while the proposed motion adapter is lightweight, our pipeline increases model size and is slower than other compact models. Additional multi-attribute limitations and bad cases are discussed in the supplementary materials.

Conclusion. We present *ACMo*, an effective architecture for multimodal, multi-attribute controllable motion generation. It uses the *Attribute Diffusion Model* for text-

to-motion generation, introduces the *Motion Adapter* for stylized motion prompts, and integrates trajectory control. The introduced *LLM Planner* can map unseen attributes into dataset text. Extensive experiments and ablation studies across multiple datasets validate their effectiveness.

References

- [1] Kfir Aberman, Yijia Weng, Dani Lischinski, Daniel Cohen-Or, and Baoquan Chen. Unpaired motion style transfer from video to animation. *ACM Transactions on Graphics (TOG)*, 39(4):64–1, 2020. 3
- [2] Fan Bao, Chongxuan Li, Yue Cao, and Jun Zhu. All are worth words: a vit backbone for score-based diffusion models. In *NeurIPS 2022 Workshop on Score-Based Methods*, 2022. 4
- [3] Haoye Cai, Chunyan Bai, Yu-Wing Tai, and Chi-Keung Tang. Deep video generation, prediction and completion of human action sequences. In *Proceedings of the European conference on computer vision (ECCV)*, pages 366–382, 2018. 2
- [4] Ling-Hao Chen, Wenxun Dai, Xuan Ju, Shunlin Lu, and Lei Zhang. Motionclr: Motion generation and training-free editing via understanding attention mechanisms. *arxiv:2410.18977*, 2024. 3, 4, 5
- [5] Xin Chen, Biao Jiang, Wen Liu, Zilong Huang, Bin Fu, Tao Chen, and Gang Yu. Executing your commands via motion diffusion in latent space. In *Proceedings of the IEEE/CVF Conference on Computer Vision and Pattern Recognition*, pages 18000–18010, 2023. 2, 3, 4, 5, 6, 7
- [6] Wenxun Dai, Ling-Hao Chen, Jingbo Wang, Jinpeng Liu, Bo Dai, and Yansong Tang. Motionlcm: Real-time controllable motion generation via latent consistency model. In *European Conference on Computer Vision*, pages 390–408. Springer, 2024. 2, 3, 5, 6
- [7] Yao Feng, Jing Lin, Sai Kumar Dwivedi, Yu Sun, Priyanka Patel, and Michael J Black. Chatpose: Chatting about 3d human pose. In *Proceedings of the IEEE/CVF Conference on Computer Vision and Pattern Recognition*, pages 2093–2103, 2024. 2, 3
- [8] Kehong Gong, Dongze Lian, Heng Chang, Chuan Guo, Zihang Jiang, Xinxin Zuo, Michael Bi Mi, and Xinchao Wang. Tm2d: Bimodality driven 3d dance generation via music-text integration. In *Proceedings of the IEEE/CVF International Conference on Computer Vision*, pages 9942–9952, 2023. 2
- [9] Chuan Guo, Xinxin Zuo, Sen Wang, Shihao Zou, Qingyao Sun, Annan Deng, Minglun Gong, and Li Cheng. Action2motion: Conditioned generation of 3d human motions. In *Proceedings of the 28th ACM International Conference on Multimedia*, pages 2021–2029, 2020. 2, 3
- [10] Chuan Guo, Xinxin Zuo, Sen Wang, Shihao Zou, Qingyao Sun, Annan Deng, Minglun Gong, and Li Cheng. Action2motion: Conditioned generation of 3d human motions. In *Proceedings of the 28th ACM International Conference on Multimedia*, pages 2021–2029, 2020. 5
- [11] Chuan Guo, Shihao Zou, Xinxin Zuo, Sen Wang, Wei Ji, Xingyu Li, and Li Cheng. Generating diverse and natural 3d human motions from text. In *Proceedings of the IEEE/CVF Conference on Computer Vision and Pattern Recognition*, pages 5152–5161, 2022. 2, 3, 5, 6
- [12] Chuan Guo, Yuxuan Mu, Muhammad Gohar Javed, Sen Wang, and Li Cheng. Momask: Generative masked modeling of 3d human motions. In *Proceedings of the IEEE/CVF Conference on Computer Vision and Pattern Recognition*, pages 1900–1910, 2024. 2, 3, 5, 6
- [13] Chuan Guo, Yuxuan Mu, Xinxin Zuo, Peng Dai, Youliang Yan, Juwei Lu, and Li Cheng. Generative human motion stylization in latent space. *arXiv preprint arXiv:2401.13505*, 2024. 3
- [14] Félix G Harvey, Mike Yurick, Derek Nowrouzezahrai, and Christopher Pal. Robust motion in-betweening. *ACM Transactions on Graphics (TOG)*, 39(4):60–1, 2020. 2
- [15] Jonathan Ho and Tim Salimans. Classifier-free diffusion guidance. *arXiv preprint arXiv:2207.12598*, 2022. 5
- [16] Jonathan Ho, Ajay Jain, and Pieter Abbeel. Denoising diffusion probabilistic models. *Advances in neural information processing systems*, 33:6840–6851, 2020. 3
- [17] Yiming Huang, Weilin Wan, Yue Yang, Chris Callison-Burch, Mark Yatskar, and Lingjie Liu. Como: Controllable motion generation through language guided pose code editing. In *European Conference on Computer Vision*, pages 180–196. Springer, 2024. 3, 6
- [18] Yiheng Huang, Hui Yang, Chuanchen Luo, Yuxi Wang, Shibiao Xu, Zhaoxiang Zhang, Man Zhang, and Junran Peng. Stablemofusion: Towards robust and efficient diffusion-based motion generation framework. In *Proceedings of the 32nd ACM International Conference on Multimedia*, pages 224–232, 2024. 2, 3, 4
- [19] Deok-Kyeong Jang, Soomin Park, and Sung-Hee Lee. Motion puzzle: Arbitrary motion style transfer by body part. *ACM Transactions on Graphics (TOG)*, 41(3):1–16, 2022. 3
- [20] Biao Jiang, Xin Chen, Wen Liu, Jingyi Yu, Gang Yu, and Tao Chen. Motiongpt: Human motion as a foreign language. *Advances in Neural Information Processing Systems*, 36:20067–20079, 2023. 2, 3, 5, 6, 8
- [21] Biao Jiang, Xin Chen, Chi Zhang, Fukun Yin, Zhuoyuan Li, Gang Yu, and Jiayuan Fan. Motionchain: Conversational motion controllers via multimodal prompts. In *European Conference on Computer Vision*, pages 54–74. Springer, 2024. 2
- [22] Peng Jin, Yang Wu, Yanbo Fan, Zhongqian Sun, Wei Yang, and Li Yuan. Act as you wish: Fine-grained control of motion diffusion model with hierarchical semantic graphs. *Advances in Neural Information Processing Systems*, 36, 2024. 2, 3
- [23] Diederik P Kingma. Auto-encoding variational bayes. *arXiv preprint arXiv:1312.6114*, 2013. 3
- [24] Ning Lan, Baoshan Ou, Xuemei Xie, and Guangming Shi. Visual environment-interactive planning for embodied complex-question answering. *IEEE Transactions on Circuits and Systems for Video Technology*, 2025. 3
- [25] Junnan Li, Dongxu Li, Caiming Xiong, and Steven Hoi. Blip: Bootstrapping language-image pre-training for unified

- vision-language understanding and generation. In *International conference on machine learning*, pages 12888–12900. PMLR, 2022. 2
- [26] Ruilong Li, Shan Yang, David A Ross, and Angjoo Kanazawa. Ai choreographer: Music conditioned 3d dance generation with aist++. In *Proceedings of the IEEE/CVF International Conference on Computer Vision*, pages 13401–13412, 2021. 2
- [27] Jinpeng Liu, Wenxun Dai, Chunyu Wang, Yiji Cheng, Yansong Tang, and Xin Tong. Plan, posture and go: Towards open-vocabulary text-to-motion generation. In *European Conference on Computer Vision*, pages 445–463. Springer, 2024. 2, 3
- [28] Zhenguang Liu, Shuang Wu, Shuyuan Jin, Shouling Ji, Qi Liu, Shijian Lu, and Li Cheng. Investigating pose representations and motion contexts modeling for 3d motion prediction. *IEEE transactions on pattern analysis and machine intelligence*, 45(1):681–697, 2022. 2
- [29] Naureen Mahmood, Nima Ghorbani, Nikolaus F. Troje, Gerard Pons-Moll, and Michael J. Black. Amass: Archive of motion capture as surface shapes. In *The IEEE International Conference on Computer Vision (ICCV)*, 2019. 5
- [30] Ian Mason, Sebastian Starke, and Taku Komura. Real-time style modelling of human locomotion via feature-wise transformations and local motion phases. *Proceedings of the ACM on Computer Graphics and Interactive Techniques*, 5(1):1–18, 2022. 2, 5
- [31] Jianmo Ni, Gustavo Hernandez Abrego, Noah Constant, Ji Ma, Keith B Hall, Daniel Cer, and Yinfei Yang. Sentence5: Scalable sentence encoders from pre-trained text-to-text models. *arXiv preprint arXiv:2108.08877*, 2021. 2, 3
- [32] Mathis Petrovich, Michael J Black, and Gül Varol. Action-conditioned 3d human motion synthesis with transformer vae. In *Proceedings of the IEEE/CVF International Conference on Computer Vision*, pages 10985–10995, 2021. 2, 3
- [33] Mathis Petrovich, Michael J Black, and Gül Varol. Temos: Generating diverse human motions from textual descriptions. In *European Conference on Computer Vision*, pages 480–497. Springer, 2022. 5
- [34] Alec Radford, Jong Wook Kim, Chris Hallacy, Aditya Ramesh, Gabriel Goh, Sandhini Agarwal, Girish Sastry, Amanda Askell, Pamela Mishkin, Jack Clark, et al. Learning transferable visual models from natural language supervision. In *International conference on machine learning*, pages 8748–8763. PmLR, 2021. 2
- [35] Gerard Salton and Christopher Buckley. Term-weighting approaches in automatic text retrieval. *Information processing & management*, 24(5):513–523, 1988. 4
- [36] Jiaming Song, Chenlin Meng, and Stefano Ermon. Denoising diffusion implicit models. *arXiv preprint arXiv:2010.02502*, 2020. 3
- [37] Zeyi Sun, Ye Fang, Tong Wu, Pan Zhang, Yuhang Zang, Shu Kong, Yuanjun Xiong, Dahua Lin, and Jiaqi Wang. Alpha-clip: A clip model focusing on wherever you want. In *Proceedings of the IEEE/CVF Conference on Computer Vision and Pattern Recognition*, pages 13019–13029, 2024. 2
- [38] G Tevet, S Raab, B Gordon, Y Shafir, D Cohen-Or, and AH Bermano. Human motion diffusion model. *arXiv preprint arXiv:2209.14916*, 2022. 2, 3, 4, 6
- [39] Aaron Van Den Oord, Oriol Vinyals, et al. Neural discrete representation learning. *Advances in neural information processing systems*, 30, 2017. 3
- [40] Mingjie Wei, Xuemei Xie, Yutong Zhong, and Guangming Shi. Learning pyramid-structured long-range dependencies for 3d human pose estimation. *IEEE Transactions on Multimedia*, 2025. 2
- [41] Zeqi Xiao, Tai Wang, Jingbo Wang, Jinkun Cao, Wenwei Zhang, Bo Dai, Dahua Lin, and Jiangmiao Pang. Unified human-scene interaction via prompted chain-of-contacts. In *The Twelfth International Conference on Learning Representations*, 2024. 3
- [42] Yiming Xie, Varun Jampani, Lei Zhong, Deqing Sun, and Huaizu Jiang. Omnicontrol: Control any joint at any time for generation. *arXiv preprint arXiv:2310.08580*, 2023. 2, 3, 4, 5
- [43] Hu Ye, Jun Zhang, Sibio Liu, Xiao Han, and Wei Yang. Ip-adapter: Text compatible image prompt adapter for text-to-image diffusion models. *arXiv preprint arXiv:2308.06721*, 2023. 2, 3, 4, 5
- [44] Lvmin Zhang, Anyi Rao, and Maneesh Agrawala. Adding conditional control to text-to-image diffusion models. 3
- [45] Mingyuan Zhang, Zhongang Cai, Liang Pan, Fangzhou Hong, Xinying Guo, Lei Yang, and Ziwei Liu. Motiandiffuse: Text-driven human motion generation with diffusion model. *arXiv preprint arXiv:2208.15001*, 2022. 3, 6
- [46] Mingyuan Zhang, Xinying Guo, Liang Pan, Zhongang Cai, Fangzhou Hong, Huirong Li, Lei Yang, and Ziwei Liu. Remodiffuse: Retrieval-augmented motion diffusion model. In *Proceedings of the IEEE/CVF International Conference on Computer Vision*, pages 364–373, 2023. 2, 3, 6
- [47] Lei Zhong, Yiming Xie, Varun Jampani, Deqing Sun, and Huaizu Jiang. Smoodi: Stylized motion diffusion model. In *European Conference on Computer Vision*, pages 405–421. Springer, 2024. 2, 3, 4, 5, 8
- [48] Zixiang Zhou, Yu Wan, and Baoyuan Wang. Avatargpt: All-in-one framework for motion understanding planning generation and beyond. In *Proceedings of the IEEE/CVF Conference on Computer Vision and Pattern Recognition*, pages 1357–1366, 2024. 2, 3, 5

Supplementary Materials for ACMo: Attribute Controlable Motion Generation

Contents

1	Visualization	
2	Experimental Design Details	
2.1	Research motivation	1
2.2	Training details	3
2.3	Trajectory ControlNet	4
2.4	Training Loss	4
2.5	Stack Layers Design	5
2.6	Classifier-free diffusion guidance	5
3	Additional Experiments	
3.1	Comparasion of VAE	5
3.2	Comparison experiment of Trajectory	5
4	Dataset process Details	
5	Metrics Introduction	
6	Limitations	
7	LLM Planner Details	
7.1	prompt	8
7.2	Frequent Word Bank	9

1 Visualization

We have tried different types of visualization methods in this section. The following are the visualizations of our three core contributions:

Reasoning motion generation. We supplemented some reasoning generation visualization with Attribute Diffusion model and LLM Planner in Fig. 1.

Stylized motion generation. We supplemented some stylized generation visualization via Motion Adapter in Fig. 2.

Text-to-motion generation. We supplemented extensive text-to-motion generation visualization with Attribute Diffusion Model in Fig. 3.

2 Experimental Design Details

2.1 Research motivation

We are hoping to create an end-to-end controllable generation application, meaning that anyone can get the motions they wish for. This faces the challenges of being difficult to control and having a generalization problem that goes beyond the dataset. So the core idea is to quickly fine-tune the model to 'see' new patterns or convert unseen descriptions to dataset-specific text.

The origin of the LLM Planner was an application where we wanted to "jump into the well," but we found that the model didn't understand the context (*i.e.* well). We thought and analyzed this precision paradox. The text in HumanML3D is so clean that it is difficult for users to interact with. Higher and higher aligned SOTA will only limit the training sample distribution to clean datasets.

The reason for the research of Motion Adapter is that we found that many motions are actually not in the HumanML3D dataset, especially in some games and movies, there are a lot of missing actions (e.g., fly) and unique character styles (e.g., superman). So, we wanted to get some stylized generated motions. Fortunately, 100STYLE has some new styles and actions that can be used as data for research samples. Finally, we are compatible with Trajectory ControlNet to implement control of multiple attributes.

Figure 1: Visual experiment of Reasoning motion generation. The proposed LLM Planner can convert unseen attributes to a dataset-specific text. The BVH production process in Momask[3] was used for visualization.

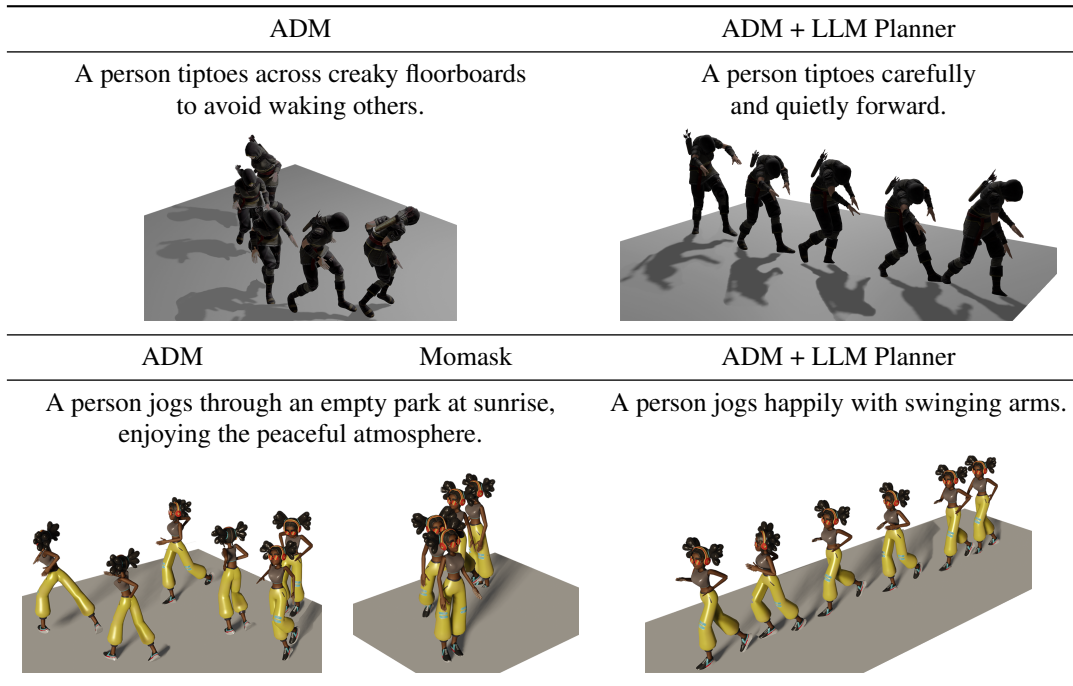


Figure 2: Visual experiment of stylized text-to-motion generation.

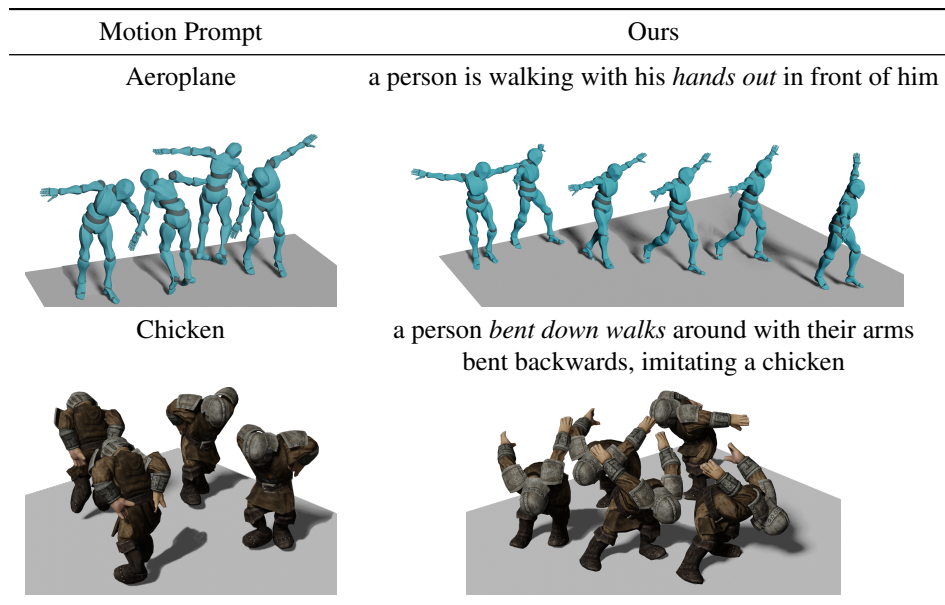
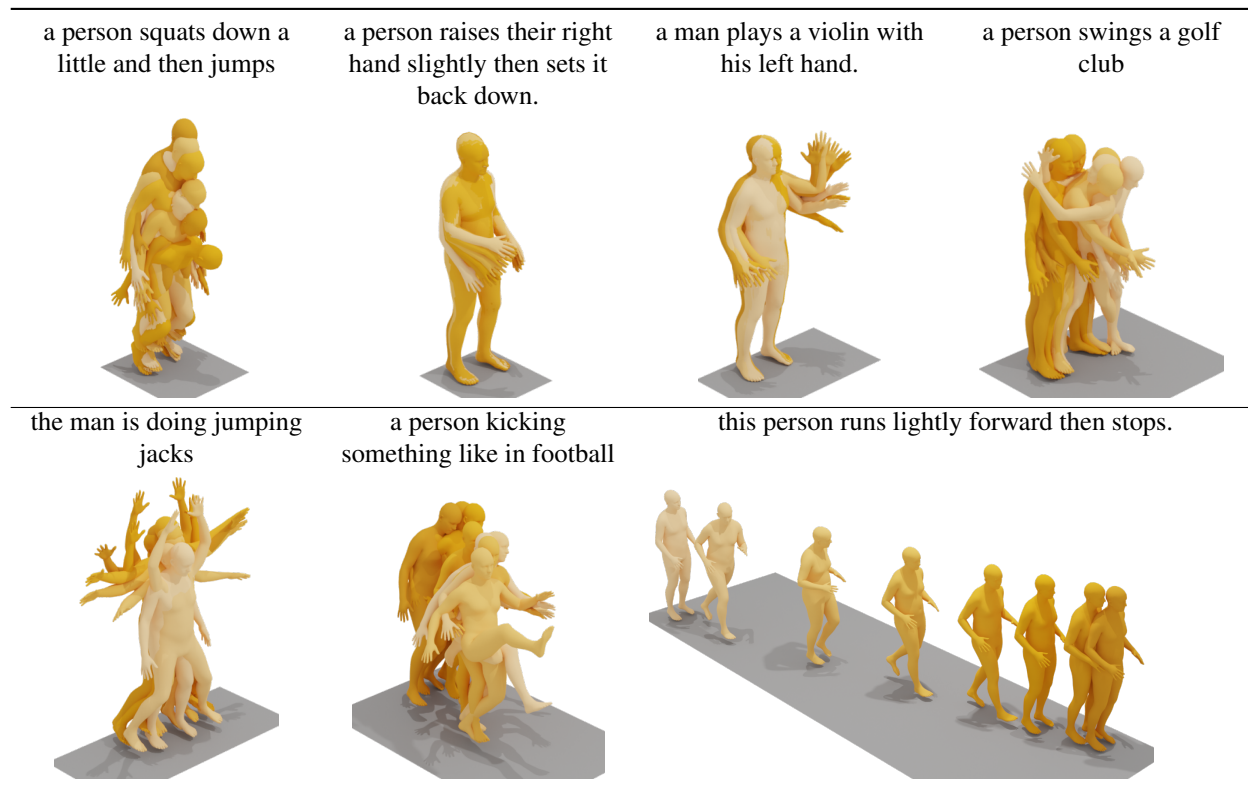


Figure 3: Visual experiment of text-to-motion generation. The proposed Attribute Diffusion Model can achieve word-level granularity generation.



2.2 Training details

Training diagram. We provided validation data for FID and R Precision when we trained the ADM, as shown in the Fig. 4. Then, we provided validation data for FID and R Precision from 1 to 1000 epochs with only self attention when we trained the Motion Adapter, as shown in the Fig. 5.

Parameters of each module. The number of model parameters for our entire network is shown in the Table 1. Because Controlnet-based models require an initial duplication of the denoiser, followed by the incorporation of control information via zero convolutions. This highlights the superiority of our motion adapter, which directly integrates into the denoiser and achieves control conditions through network parameter reuse and the addition of a few attention layers. And our approach doesn't require train-

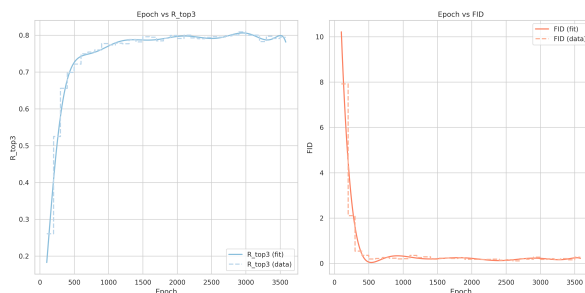


Figure 4: Training ADM detail diagram.

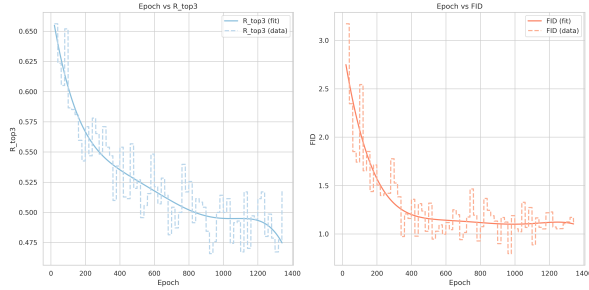


Figure 5: Finetuning self-attention detail diagram. This illustrates the overfitting phenomenon that results as the epoch learns. The pre-trained alignment knowledge of motion and text is severely lost.

ing an style encoder. We used the trained VAE directly as the style encoder because they are both motion mode.

Modular	text encoder	vae	denoiser	controlnet	traj_encoder
Param.	335 M	18.0 M	29.8 M	30.7 M	7.8 M

Table 1: Model parameters for different modules.

Inference Tips. To better replicate our results in each table, we offer some tips. The random number seed of all experiments was set to 1234, and then the batchsize during test was 32, the guidance scale was adjusted according to the tables, and two A6000 were used. The above parameters are the main factors that affect the different effects of the same training weight.

Therefore, we recommend that when using the demo, generate multiple identical text inputs (e.g. eight same texts) at the same time, so as to construct a batch to produce better results. Meanwhile, the descriptions of the text, style, and trajectory should be as consistent as possible, without any conflict (e.g., 'bent' in the text and 'old' for the style complement each other well).

2.3 Trajectory ControlNet

In our Trajectory ControlNet, we only design a simple ControlNet to verify the compatibility of the Motion Adapter and ControlNet to achieve multi-mode control. We have found that guided diffusion model control can be very time consuming, even if it works well. This is

the opposite of the lightweight and fast design of our motion adapter. Specifically, our ControlNet design is shown in the Figure 6. Training the Trajectory ControlNet for 1000 epochs takes approximately 24 hours without Control loss, and roughly 48 hours with control loss.

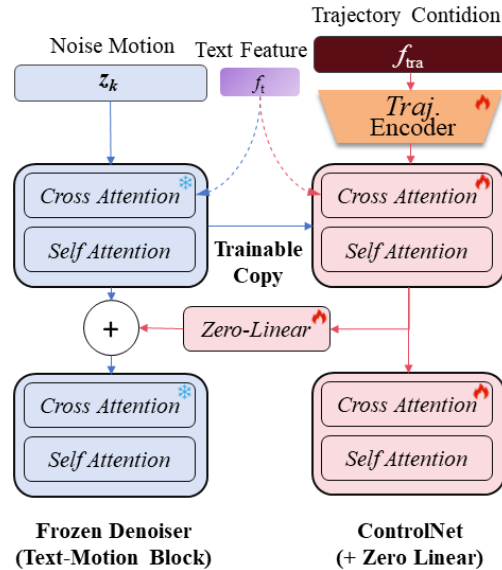


Figure 6: Finetuning self-attention detail diagram. This illustrates the overfitting phenomenon that results as the epoch learns. The pre-trained alignment knowledge of motion and text is severely lost.

2.4 Training Loss

The train loss of our work follows the MLD [1] implementation. We only trained with text conditions in Stage 1. In Stage 2, the model are finetuned through other datasets, is still trained with text as a condition. In Stage 3, the condition consists of text and trajectories. The proposed Motion Adapter and ControlNet aligns with the training loss L_{ADM} of diffusion model.

However, we found that when training ControlNet, the loss constraint only in the latent space is not strong enough. This can provide a trajectory guidance rather than a mandatory trajectory. Although as a verification of compatibility, it is enough. Following [2], we tried to set a control loss, a l_2 loss in original space after vae de-

code, but the model did not converge well, we are trying to solve it.

2.5 Stack Layers Design

In the proposed attribute diffusion model, we conducted ablation studies on stacked layers to explore whether the learning of text and motion should be alternated. Specifically, we designed experiments stacking motion self-attention and text cross-attention, as illustrated in the Fig. 7. Our findings validate the effectiveness of decoupling the text-to-motion block.

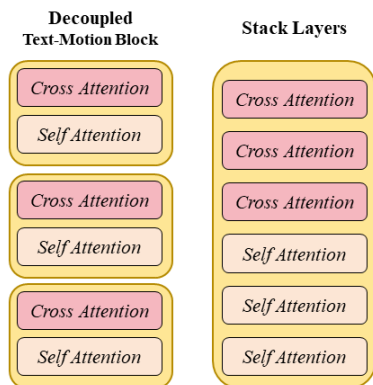


Figure 7: Finetuning self-attention detail diagram. This illustrates the overfitting phenomenon that results as the epoch learns. The pre-trained alignment knowledge of motion and text is severely lost.

2.6 Classifier-free diffusion guidance

Our denoiser g is trained with classifier-free diffusion guidance, learning both the conditioned and unconditioned distributions. A linear combination of these is used as follows:

$$g_{\theta,w}^{\text{cfg}}(z_t, t, c) = wg_{\theta}(z_t, t, c) + (1-w)g_{\theta}(z_t, t, \emptyset),$$

$$\{f_t, f_m, f_{\text{tra}}\} \in c, \quad (1)$$

where c represents the conditions (*i.e.*, the feature of texts f_t , motion prompt f_m and trajectories f_{tra}), and w is the

guidance scale. A value of $w > 1$ strengthens the guidance effect. This approach effectively balances the trade-off between boosting sample quality and reducing diversity in conditional diffusion models.

3 Additional Experiments

3.1 Comparison of VAE

By adjusting the parameter configuration of MLD-1, we achieved the VAE results for our VAE-7. The primary modification involved setting the size of the latent space to 7. This adjustment was based on previous experiments within the MLD framework, which demonstrated that a latent space size of 7 yields the most realistic VAE results.

As shown in Table 2, we compared our approach with all current state-of-the-art VAE methods in terms of motion reconstruction performance, where VAE reconstruction error is evaluated by MPJPE and PAMPJPE, measuring errors in millimeters. This demonstrates that our motion representation space is the most faithful to real motion, thereby preserving more kinematic details.

Table 2: Evaluation of our motion encoder on the motion part of HumanML3D dataset. We follow [6] to evaluate our VAE model E . MPJPE and PAMPJPE are measured in millimeter. Compared to other motion codecs, our method is obviously closer to the most realistic data.

Method	Motion Reconstruction			
	MPJPE↓	PAMPJPE↓	FID↓	DIV→
Real	-	-	0.002	9.455
TM2T [5]	230.1	-	0.307	-
ACTOR [8]	65.3	41.0	0.341	9.569
MLD-1 [1]	54.4	41.6	0.247	9.630
MotionGPT [6]	55.8	40.1	0.067	9.675
MoMask [3]	29.5	21.9	0.019	9.609
Ours	12.8	8.7	0.007	9.530

3.2 Comparison experiment of Trajectory

As shown in Table 3, our experiments validate ControlNet’s effectiveness in latent space under L_{ADM} , demonstrating that trajectory-guided motion effectively reduces positional errors by aligning poses with trajectories. While it underperforms compared to state-of-the-art

trajectory-based methods, likely due to insufficient latent space loss constraints, this outcome sufficiently verifies the compatibility between our proposed Motion Adapter and Trajectory ControlNet.

Table 3: Evaluation of our trajector controlnet. ‘‘LC’’ and ‘‘MC’’ refer to the control supervision introduced in the latent space and motion space. It shows that our trajectory control can provide enough trajectory guidance.

Method	Traj.err.↓ (50cm)	Loc.err.↓ (50cm)	Avg.err.↓ (50cm)
OmniControl (MC)	0.3362	0.0322	0.0977
MotionLCM (LC&MC)	0.1960	0.0143	0.1092
Ours w/o Control	0.6208	0.4024	0.8201
Ours (LC) w/ Control	0.5498	0.3341	0.5872

4 Dataset process Details

HumanML3D dataset. Thanks to the data processing work of [4], we identified several annotation errors in HumanML3D as well as instances of misspelled words. We did not address the annotation errors, but the LLM Planner provides an excellent solution for correcting spelling mistakes. For the ‘left,right,clockwise’ orientation of the current model, *we found that there are certain annotation errors in the dataset, especially ‘left’‘right’*. *We haven’t solved it yet, for a fair comparison, but we think it’s the key to the puzzle model.*

100STYLE dataset. Thanks to the data processing work of [9], we found that there are some retargeted actions missing in the dataset, including WhirlArms, WideLegs, WiggleHips, WildArms, WildLegs, and Zombie. We directly removed the data for these actions, approximately one thousand entries, and fine-tuned the model using the remaining 15,000 or so entries. The difference is that we re-conducted the training and testing split of the dataset. Smoodi was trained by mixing two datasets to maintain the original knowledge, while we only fine-tuned on the new dataset. The smaller reduction in our R Precision illustrates the superiority of our fine-tuning approach. Of course, this also led to a certain amount of text and motion alignment knowledge forgotten, we are also trying to mix the original data to fine-tune.

Motion Representations. We unify all dataset input representations as HumanML3D via the tools provided by [4], then obtain latent vector representations in latent space through VAE, and finally use SMPL [7] format and BVH for visualization and application.

5 Metrics Introduction

Rule Consistency Score ($RCS \in \{0, 1\}$) measures strict rule compliance in generated instructions, as dataset alignment depends on this consistency. LLM as binary evaluator determines the model results, and then calculates the correct rate:

$$RCS = \frac{1}{n} \sum_{i=1}^n \{f(I_{model}^i) == True\}, \quad (2)$$

where n denotes the number of answer; f is LLM as a judge function, with the value of boolean True or False; I_{model}^i is the instruction of i -th model. RCS results range 0 – 100%.

Plan Score ($PS \in [1, 5]$) measures the relative scores of five large language models. We obtain the scores of each model by ranking these methods. The closer the model is to 1, the higher the ranking is, and the better balance between real instructions and rules is achieved. Our Plan Score is the average score of different instructions:

$$PS = \frac{1}{n} \sum_{i=1}^n f(I_{user}; I_{model}^i), \quad (3)$$

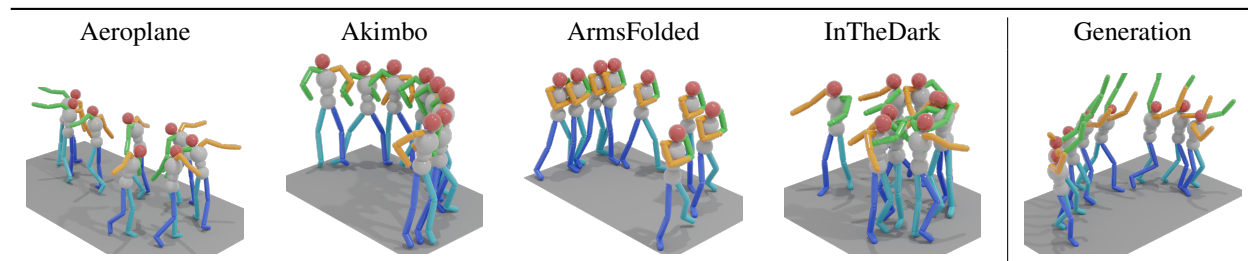
where I_{user} denotes the origin instruction for reference; f is LLM as a sort function, with the value of an integer from 1 to 5; I_{model}^i is the instruction of i -th model.

6 Limitations

We honestly discuss any limitations encountered during the research and hope to discuss and resolve them in the future. We would like to call for recognition of some new limitations, which will also give more inspiration to the research field. Finally, we hope that it does not affect the innovation of our work.

Motion generation for long texts. This limitation comes from our evaluation of the MotionIT dataset, where

Figure 8: An example illustrates the bad case. All auto text annotations are 'a person moves around with their arms outstretched.' This leads to the interference of the text information, making the stylized generated results random.



we found that existing methods do not work well for the generation of long text stories. For example: "A person parkour-flips over a sinking river ferry's railings, dodging panicked passengers, to restart engines before currents drag it into a waterfall." The result after llm planner is: "A person flips over railings quickly, dodges passengers, and runs forward to start urgently." The bad case is shown as Fig. 9. We find that such an motion sequence contains multiple actions that need to be generation, and inevitably exists information that is not present in the dataset. In addition, move range in the motion is wide and the generation time is long, which brings great challenges to the existing motion generation.

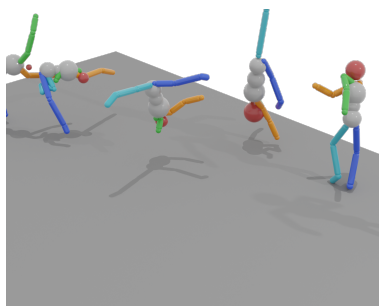


Figure 9: A bad case of 'A person parkour-flips over a sinking river ferry's railings, dodging panicked passengers, to restart engines before currents drag it into a waterfall.' Long text, long move range, long time and zero-shot generation are very difficult.

Foot Skating. The foot skating cause of this was the finetuning we did on the new data set. However, the mean and variance of different datasets (HumanML3D

and 100STYLE) are different, which will lead to incorrect normalization, thus resulting in the visualization of foot skating. We consider that any training with multiple datasets may encounter this problem. We will solve it in the future.

Multi-condition conflicts in motion synthesis. Multiple control conditions (e.g., style, text, trajectory) may induce optimization conflicts that compromise motion stability. We found the same problem with other methods [9], requires repeated parameter adjustment and multiple generation to get desired motion. Explicit contradictions between semantic (text) and kinematic (style/trajectory) constraints particularly risk yielding unpredictable outcomes.

Our modular architecture, while offering interpretability and selective condition application through decoupled components, inherits fundamental limitations of multi-objective optimization - specifically reduced stability under conflicting multi-condition inputs.

We analyze that the conflict between style and text is may caused by automatic text annotation. Because current automated text annotations make it easy to get the same text description for all types of actions, a text-style generated motion is actually derived from the supervised action category, as shown in Fig. 8. This is most likely one of the difficulties that led to the current generation of multiple conditions.

7 LLM Planner Details

In our experiment, we utilized ChatGPT-4o and deepseek-r1 to create the MotionIT dataset and implemented LLM

Planner using various large models. Finally, we used a deployed deepseek-r1-32b as the critic for evaluation. The following are our prompts and implementation details.

Frequent Word Bank: right forward ...
Now input is : ...

7.1 prompt

GPT-4o/Deepseek Prompt (Data Generation)
You are now a motion analysis assistant. I need you to generate descriptions of physical body actions that require reasoning. Direct actions include walking, running, jumping, etc. Actions requiring reasoning involve additional context or attributes, such as walking after a paper is accepted or running to help a child who has fallen.

- Focus solely on full-body physical actions, avoiding facial expressions or hand details.
- Begin each description with “a person.”

Please provide 100 different descriptions of physical body actions. Each description should be about 15 words. Ensure the descriptions are concise and clear!
Example:
a person walks nervously towards a podium to deliver an important speech at a conference.

We ensured the diversity of the generated results through human observation and simple adjustments to the prompt, which we generated every 100 examples in a group and collected 5K datasets. This dataset will be made public.

Prompt (As LLM Planner)
Act as a motion analysis agent that translates complex action instructions into simplified text commands from Frequent Word Bank. You need to consider whether the context is a necessary output, as the Frequent Word Bank usually does not contain context-related words. Maintain sentence fluency while following these rules:

1. Strictly start outputs with “A person” in English
2. Keep sentences concise - describe actions/characteristics minimally. Focus on the action and the character of the action itself.
3. The actions described need to have distinguishing features, such as happy, left hand raised, etc
4. Prioritize the use of words from the Frequent Word Bank (listed below), especially verbs, when appropriate
5. Output ONLY the final sentence without explanations

Examples Output:
a person walking backwards slowly
a man raises its right arm and wiggles it and brings it back down
Example:
User: A person is walking when his paper is accepted
Agent: A man walks happily and relaxed with swinging arms.

Deepseek-r1-32B Prompt (For Rule Judgement)
Act as a rule-based validator for motion descriptions. Return ‘True’ or ‘False’ with JSON based on strict compliance with these 5 non-negotiable criteria:

1. Initial Phrase Enforcement Output MUST start with exactly “A person” or “a person” (case-sensitive match)
2. Structural Integrity MUST be a single continuous sentence MUST contain NO explanations, context, or examples
3. Attribute Requirement MUST include ≥ 1 explicit distinguishing attribute (adverb/adjective: e.g., ‘quickly’, ‘left hand’, ‘diagonally’) The result should focus on the action itself, not the context information.
4. Lexical Compliance $\geq 50\%$ of verbs/body parts MUST come from the Frequent Word Bank
5. Grammatical Soundness MUST maintain grammatical correctness and action fluency

Validation Protocol:
{ “validation_result”: { “final_result”: “False”, // This should be ‘True’ only if all criteria are satisfied “final_explanation”: “Not all criteria were met. Specifically, Criterion 1 failed because [brief reason].” } }

Examples: User: “A person jumps” Output: { “validation_result”: { “final_result”: “False”, “final_explanation”: “Violates Criteria 3 that ...” } }

User: “A person runs energetically through the rain, unfazed by the downpour soaking them.” Output: { “validation_result”: { “final_result”: “False”, “final_explanation”: “Not all criteria were met. Specifically, Criterion 2 failed because the sentence contains context ...” } }

User: “a person raises right arm and spins clockwise” Output: { “validation_result”: { “final_result”: “True”, “final_explanation”: “All pass because ...” } }

Deepseek-r1-32B Prompt (For Plan Score Judgement)
Act as an expert evaluator for motion description generation models. Your task is to rank outputs from 5 different models based on their adherence to specifications and information preservation. The result should focus on the action itself, not the context information.

Evaluation Criteria (Descending Priority):

1. ****Format Compliance****: - Must start with “A person” - Must output ONLY the final sentence. MUST contain NO explanations, context, or examples - Must be in English - Keep sentences concise - describe actions/characteristics minimally, focusing on the action and the character of the action itself - Prioritize the use of words from the Frequent Word Bank (listed below), especially verbs, when appropriate

2. **Content Quality**: - Contains distinguishing characteristics/attributes (e.g., body parts, emotions, directions) - Maintains all key information from original instruction - Prioritizes words from Frequent Word Bank

3. **Linguistic Quality**: - Concise and fluent expression - No redundant contextual information - Grammatically correct structure

Task Description: You will receive: 1. Original user instruction
2. 5 model outputs (labeled A-E)

Required Output Format: Rank the models from best to worst (1-5), where 1 is the best and 5 is the worst. Provide explanations for each model's score based on the criteria. **YOU MUST OUTPUT THE sorted LIST!** Your sorted list must match the explanation! JSON Format!

Example Output: { "sorted_list": ["A", "D", "B", "C", "E"], "explanation": { "A": "Explanation for rank 1", "D": "Explanation for rank 2", "B": "Explanation for rank 3", "C": "Explanation for rank 4", "E": "Explanation for rank 5" } }

We tried evaluating with different models, but we found significant variations in the evaluation results when using different models, such as various versions of Qwen2.5. Finally, thanks to the role of the thought chain, we chose Deepseek-r1 as the large evaluation model. Its output thought chain process can effectively and more credibly judge the accuracy of the results.

7.2 Frequent Word Bank

The word bag of the first 512 high-frequency words in HumanML3D. We adopted TF-IDF to calculate our bag of words, the core code in the listing. The answer of the wordbag is shown in Table 4.

```

1 from sklearn.feature_extraction.text import
  TfidfVectorizer
2 vectorizer = TfidfVectorizer(max_features=1024,
  stop_words='english')
3 tfidf_matrix = vectorizer.fit_transform(
  documents)
4 words = vectorizer.get_feature_names_out()
5 # Sum the columns to get the total TF-IDF score
  for each word
6 tfidf_scores = tfidf_matrix.sum(axis=0).A1
7 word_tfidf = list(zip(words, tfidf_scores))
8 # sort and obtain 512 important words
9 important_words = sorted(word_tfidf, key=lambda
  x: x[1], reverse=True)[:1024]

```

Listing 1: TF-IDF codes

Table 4: Frequent Word Bank. This recorded 512 high-frequency words from the HumanML3D dataset, which were used as Prompt inputs in the LLM to allow the large model to understand the text information in the dataset.

right	forward	left	hand	walk	arm	step
slowly	leg	circle	head	turn	foot	backwards
stand	jump	motion	place	straight	slightly	clockwise
raise	object	sit	face	body	ground	run
stop	quickly	wave	throw	hold	knee	pick
line	bend	lift	direction	knee	kick	air
jog	dance	start	pace	look	chest	shoulder
bent	balance	squat	floor	jumping	stretch	make
lean	knees	sides	swing	spot	push	backward
reach	legs	small	running	elbow	appear	diagonally
bring	hop	way	grab	hip	stair	cross
level	shake	waist	clap	punch	using	crawl
dancing	jack	touch	gesture	high	carefully	wide
end	chair	stick	thing	near	pose	spin
half	casually	extend	room	opposite	uses	drink
crouch	big	upper	catch	mouth	raising	uses
little	shape	come	wrist	lifting	weight	hips
apart	taking	continue	places	pushed	stance	path
drop	point	begin	quick	curve	try	fall
stopping	rotate	center	open	couple	perform	upwards
watch	table	scratch	manner	kneel	climb	angle
play	bow	crosses	hit	spread	pull	exercise
shuffle	outward	crawls	movement	warm	twist	box
wipe	rail	surface	motions	short	steady	speed
support	shakes	facing	torso	upward	ahead	basketball
gently	kicking	cartwheel	squatting	shelf	leaning	trying
long	dances	swaying	wall	area	elbows	rub
curved	middle	punches	touches	briskly	wheel	forearm
complete	crouches	gestures	screen	degrees	act	lightly
upright	neck	sets	swimming	boxing	rest	extended
bottle	playing	golf	dumbbell	suddenly	bounce	sidestep
stomach	shaking	started	outstretched	guitar	door	rotates
shuffles	check	wash	handrail	camera	moment	arc
picking	downward	railing	kneels	seat	clean	close
shift	limp	dodge	cat	balancing	clapping	quarter
avoid	hopping	repeats	overhead	lunge	dog	stay
hunch	performs	crouched	pour	steering	scratches	slide
skip	karate	pivot	briefly	catches	thigh	leap
crossing	sidesteps	stride	sprint	trip	pause	grabbed
bows	toe	plane	reaching	land	alternate	placing
pretend	flap	lay	swim	salsa	zig	drinking
fours	crouching	roll	football	help	confidently	completely
hard	semi	hunched	waltz	pain	rubs	tilt
acting	stool	length	action	relaxed	recover	curl
fight	march	moved	fist	cautiously	oval	downwards
twists	spinning	pivots	rapidly	ramp	window	stagger
grabbing	clock	obstacle	washing	wiping	heel	stagger
march	clasp	slope	returning	palm	proceeds	distance
gap	elevated	pauses	stationary	eating	rotating	bicep
horizontally	ladder	stir	trips	crossed	uneven	toes
zigzag	higher	jumped	edge	scratching	ankle	simultaneously
shoe	bringing	shifts	inward	stroke	ballet	lowering
happily	partner	pushing	food	hurt	opens	various
lead	style	leading	carry	location	weights	keeping
talk	space	hang	defensive	container	stumbling	follow
drag	wiggle	aggressively	falls	horizontal	brush	fastly
sweeping	beginning	slides	form	tap	semicircle	dribble
toss	bounces	coming	posture	alternating	flight	practice
lunges	tie	clasps	padding	uppercut	stretched	balances
rock	rubbing	chin	neutral	resting	pulls	lands
objects	flex	swat	finger	wind	parallel	random
extending	warming	keeps	similar	lose	cleaning	thighs
infront	viewer	single	round	water	outwards	club
abruptly	mix	came	block	stomp	vertically	press
glass	light	far	jab	lap	stiff	stiff
drive	tries	movements	exercises	hello	terrain	gait
swifly	eye	shot	veer	signal	type	wobble
wait	zombie	leaps	woman	straighten	rolls	sneak
mid	continuously	duck	landing	work	backs	tilts
imitate	bowl	pours	handstand	catching	row	tip
cover	tight	pass	steadily	acts	pretending	crowd
dry	salute	exercising	width	talking	centre	ends
vigorously	brisk	belly	shrug	strides	flip	recovers
overhand						

References

- [1] Xin Chen, Biao Jiang, Wen Liu, Zilong Huang, Bin Fu, Tao Chen, and Gang Yu. Executing your commands via motion diffusion in latent space. In *Proceedings of the IEEE/CVF Conference on Computer Vision and Pattern Recognition*, pages 18000–18010, 2023. [4](#), [5](#)
- [2] Wenxun Dai, Ling-Hao Chen, Jingbo Wang, Jinpeng Liu, Bo Dai, and Yansong Tang. Motionlcm: Real-time controllable motion generation via latent consistency model. In *European Conference on Computer Vision*, pages 390–408. Springer, 2024. [4](#)
- [3] Chuan Guo, Yuxuan Mu, Muhammad Gohar Javed, Sen Wang, and Li Cheng. Momask: Generative masked modeling of 3d human motions. In *Proceedings of the IEEE/CVF Conference on Computer Vision and Pattern Recognition*, pages 1900–1910, 2024. [2](#), [5](#)
- [4] Chuan Guo, Shihao Zou, Xinxin Zuo, Sen Wang, Wei Ji, Xingyu Li, and Li Cheng. Generating diverse and natural 3d human motions from text. In *Proceedings of the IEEE/CVF Conference on Computer Vision and Pattern Recognition*, pages 5152–5161, 2022. [6](#)
- [5] Chuan Guo, Xinxin Zuo, Sen Wang, and Li Cheng. Tm2t: Stochastic and tokenized modeling for the reciprocal generation of 3d human motions and texts. In *European Conference on Computer Vision*, pages 580–597. Springer, 2022. [5](#)
- [6] Biao Jiang, Xin Chen, Wen Liu, Jingyi Yu, Gang Yu, and Tao Chen. Motiongpt: Human motion as a foreign language. *Advances in Neural Information Processing Systems*, 36:20067–20079, 2023. [5](#)
- [7] Matthew Loper, Naureen Mahmood, Javier Romero, Gerard Pons-Moll, and Michael J Black. Smpl: A skinned multi-person linear model. In *Seminal Graphics Papers: Pushing the Boundaries, Volume 2*, pages 851–866. 2023. [6](#)
- [8] Mathis Petrovich, Michael J Black, and Gül Varol. Action-conditioned 3d human motion synthesis with transformer vae. In *Proceedings of the IEEE/CVF International Conference on Computer Vision*, pages 10985–10995, 2021. [5](#)
- [9] Lei Zhong, Yiming Xie, Varun Jampani, Deqing Sun, and Huaizu Jiang. Smoodi: Stylized motion diffusion model. In *European Conference on Computer Vision*, pages 405–421. Springer, 2024. [6](#), [7](#)